North Atlantic sea level budget revisited

Zhe Song[1,2], Anny Cazenave[1], William Llovel[2], Andrea Storto[3] and Marie Bouih[4]

[1]Université de Toulouse, LEGOS (CNES/CNRS/IRD/UT3), 31401 Toulouse, CEDEX 9, France
[2]Université de Bretagne Occidentale, CNRS, Ifremer, IRD, Laboratoire d'Océanographie Physique et Spatiale (LOPS), IUEM, 29280, Plouzané, France
[3]Institute of Marine Science, National Research Council of Italy, Rome, Italy
[4]Magellium, 31520 Ramonville St Agne, France

Correspondence to: Zhe Song (zhe.song@univ-brest.fr) and Anny Cazenave (anny.cazenave@univ-tlse3.fr, anny.cazenave@gmail.com)

~~Submitted to~~ Ocean Science

Revised version

11 May ~~February~~ 2026

Abstract

Based on satellite altimetry, GRACE space gravimetry and Argo-based steric data down to 2000m, recent studies have shown that the North Atlantic sea level budget (i.e., altimetry-based sea level minus sum of components) of the past two decades is not closed, with strong regional residuals in the North Atlantic. This was suggested to result from salinity errors reported since ~2015 in some Argo float measurements. In this study, we revisit the North Atlantic sea level budget, using satellite altimetry, GRACE and GRACE-FO data, different Argo products and two ocean reanalyses (CIGAR and ORAS5) over the 2004-2022 time span. The ocean reanalyses are used to estimate the manometric contribution, an alternative to using GRACE data, as well as the deep ocean contribution to the sea level budget, not yet fully sampled by Argo. Analyzing different data sets allows us to evaluate their impact on the previously reported non-closure of the North Atlantic sea level budget. We first find that using the CIGAR ocean reanalysis-based manometric component significantly reduces the residuals of the North Atlantic sea level budget compared to GRACE. We also find that accounting for the deep ocean (below 2000m) thermal expansion (using the CIGAR reanalysis) allows for 30% reduction of the North Atlantic budget residuals when using GRACE for the manometric component, while the mean residual trend is reduced by a factor of 2 when using CIGAR for the manometric sea level. In the latter case, the budget is closed within data uncertainties. –The North Atlantic halosteric component based on Argo and CIGAR in the upper 2000m displays a small decrease since the early 2010s. However, this negative trend becomes stronger after 2016. The 2010–2016 halosteric decrease may reflect a real salinity increase in the region, although salinity measurement errors may have impacted the halosteric component after that date.

1 Introduction

While many studies have been devoted to assessing the global mean sea level budget over the satellite altimetry era (1993 to present) (e.g., Barnoud et al., 2021; Bouih et al., 2025; Chen et al., 2020; Dieng et al., 2017; Horwath et al., 2022; Llovel et al., 2023; Nerem et al., 2018; WCRP, 2018) , only a few have focused on the regional sea level budget, with mixed results (e.g., Bouih et al., 2025; Camargo et al., 2023; Frederikse et al., 2016; Hamlington et al., 2020; Mu et al., 2024; Royston et al., 2020). At the global scale, the main terms of the sea level budget are the global mean sea level rise, ~~and~~ ocean mass (known as barystatic sea level, Gregory et al., 2019), and thermosteric sea level changes. At regional scale, however, other factors play a non-negligible role, such as the halosteric (i.e., salinity-related) component, which makes the regional sea level budget more complex to assess. In effect, a spurious salinity drift (giving rise to an important halosteric component decrease) has been reported recently in some Argo-based measurements (Liu et al., 2020; Ponte et al., 2021; Wong et al., 2023), that is supposed to have a strong impact on the closure assessment of the regional sea level budget. Considering all ocean basins, a recent study (Bouih et al., 2025) investigated the regional sea level trend budget closure over the 2004-2022 time span, using altimetry-based sea level data, GRACE space gravimetry for the regional ocean mass variations (also called manometric component, Gregory et al., 2019) and Argo data for the steric (sum of thermosteric and halosteric terms) component down to 2000m (global mean trends removed from all data sets). Bouih et al. (2025) also considered several ocean reanalyses to compute the manometric component (an alternative to using GRACE data), following the approach developed by Camargo et al. (2023), i.e., using the sterodynamic sea level (Gregory et al., 2019) computed by the reanalysis and correcting it for the local steric effect. The Bouih et al. (2025)'s study showed that in the Pacific, Indian and South Atlantic o~~O~~ceans, the sea level budget trend residuals (altimetry-based sea level minus sum of components) were non-significant, considering the data uncertainties. On the other hand, strong positive residuals were found in the North Atlantic, whatever the manometric

component considered (i.e., either from GRACE or from the ocean reanalyses). These authors suspected the Argo-based spurious halosteric component (impacted by the Argo-based salinity drift) as the cause of the non-closure of the sea level budget in the North Atlantic.

In the present study we revisit the question of the North Atlantic sea level budget over the 2004-2022 time span, using a variety of different data sets for the components of the sea level budget: different GRACE mascon solutions and different Argo-based gridded products down to 2000m, as well as two ocean reanalyses that provide an estimate of the steric signal from the deep ocean. Our objective is to evaluate the impact of each product on the currently reported non-closure of the North Atlantic sea level budget. An important addition, compared to the Bouih et al. (2025)'s study, ~~indeed~~ consists of accounting for the deep ocean warming below 2000m (not sampled by Argo) using estimates from the ocean reanalyses. This paper is organized as follows. Section 2 presents the data and analysis method. Section 3 displays the results for the North Atlantic sea level budget, both in terms of trend maps and time series. The sea level budget excluding the North Atlantic (average over all other oceans) is also briefly discussed in that section. A synthesis of the results is presented in the Discussion section (section ~~0~~4) with some highlights on the few main messages arising from this study.

2 Data and methods

2.1 Data

2.1.1 Altimetry-based total sea level

Sea level variations have been continuously measured by satellite altimetry since 1993. In this study, we use the daily 0.25° ×0.25° gridded sea level anomaly data, version DT2021 available from the Copernicus Climate Change Service (C3S) (https://cds.climate.copernicus.eu/). The data set is further corrected for the TOPEX-A instrumental drift that affected the first 6 years of the time series, but the correction has no impact on our assessment that starts in 2004. The

Jason-3 radiometer drift that impacts the wet troposphere correction (Brown et al., 2023) is corrected for. The altimetry data set is also corrected for the absolute Glacial Isostatic adjustment (GIA) effect, using the ICE6G-D model from Peltier et al. (2018).

2.1.2 GRACE-based ocean mass

The Gravity Recovery and Climate Experiment (GRACE) and GRACE Follow-On (GRACE-FO) are joint missions by the National Aeronautics and Space Administration (NASA) and the German Aerospace Center (DLR) (Tapley et al., 2019). These satellites have been measuring temporal variations in Earth's gravity field since 2002. This data set is essential for estimating mass redistribution in the oceans, terrestrial water storage, ice sheets, and glaciers. GRACE/GRACE-FO data are generally available in two forms: Spherical Harmonic (SH) coefficients and Mass Concentration (mascon) solutions. In this study, we utilize the latest Release 6 (RL06) mascon solutions provided by three different institutions: the Center for Space Research (CSR), the Jet Propulsion Laboratory (JPL), and the Goddard Space Flight Center (GSFC)~~German Research Centre for Geosciences (GFZ)~~. These mascon solutions, at monthly temporal resolution, are corrected for the geocentric motion (degree-1) using the Sun et al. (2016) solution. The C_{20} and C_{30} coefficients are derived from Satellite Laser Ranging (SLR) data. The GIA correction for GRACE is based on the ICE6G-D model from (Peltier et al. (2018). Additionally, the GAD product derived from AOD1B models (Dobslaw et al., 2017; Flechtner et al., 2014), which represents non-tidal atmospheric and oceanic mass redistribution, is added back over the ocean areas to restore the ocean bottom pressure, which combines the effects of ocean mass and atmospheric loading. For alignment with altimetry-based sea level data which are corrected for the inverse barometer, we remove the global mean atmospheric pressure at every grid mesh in GRACE/GRACE-FO ocean mass data using the spatial mean of the GAD product at each month (Chen et al., 2019). In this study, we ~~both~~ use the ensemble mean of~~individual~~ the three ~~their~~ mascon solutions~~ as well as their ensemble mean~~.

2.1.3 Argo-based gridded data

The Argo program is an international observational network that deploys a global array of autonomous profiling floats to measure temperature and salinity in the upper 2000m of the ocean. Several institutions process the raw data from these floats and publish gridded temperature (T) and salinity (S) data sets. In this study, we utilize three distinct gridded products: the Scripps Institution of Oceanography (SIO, Roemmich and Gilson, 2009), the Japan Agency for Marine-Earth Science and Technology (JAMSTEC, Hosoda, 2007), and the Met Office Hadley Centre (EN4 product, version 2.2, Cheng et al., 2014). Note that the SIO product rejects salinity profiles exceeding a difference of 0.1 psu when comparing to historical estimate based on the WOCE Global Hydrographic Climatology (Roemmich and Gilson, 2009). This correction tends to withdraw the salinity drift reported in Argo floats since 2016 (Liu et al., 2020; Ponte et al., 2021; Wong et al., 2023). Note that the other two products do not apply such a correction. All three data products are available at https://argo.ucsd.edu/data/data-access/ (downloaded in October 2025). The thermosteric, halosteric and total steric sea level time series are computed from these gridded temperature and salinity data using the Gibbs SeaWater (GSW) Oceanographic Toolbox (McDougall et al., 2011) which implements the 2010 Thermodynamic Equation Of Seawater (TEOS-10) standard. The gridded Argo-based time series have a spatial resolution of $1° \times 1°$ at monthly interval over January 2004 to December 2022.

2.1.4 Ocean reanalyses

We also used two ocean reanalysis data sets: (1) the CNR-ISMAR Global Historical Reanalysis (CIGAR, Storto and Yang, 2024), and (2) the Ocean Reanalysis System 5 (ORAS5, Zuo et al., 2019) available from the Copernicus Climate Change Service (https://www.copernicus.eu/en/copernicus-services).

CIGAR is a reanalysis system developed by Storto and Yang (2024). Its resolution is 1°x1°. It is based on the NEMO ocean model version 4.0.7 (https://www.nemo-ocean.eu/) and is forced by the ~~ECMWF~~ ERA5 atmospheric reanalysis from the European Center for Medium-range Weather Forecast (ECMWF) (https://www.ecmwf.int/en/forecasts/dataset/ecmwf-reanalysis-v5). The system uses a three-dimensional variational (3D-Var) scheme to assimilate in situ profiles from the EN4 data set. Notably, CIGAR does not assimilate satellite altimetry data, which allows for independent comparisons. The system consists of 32 ensemble members generated through varying configurations (e.g., perturbed initial conditions and atmospheric forcing). In this study, we use the ensemble mean of the 32 members to derive the thermosteric, halosteric and steric sea level.

The ORAS5 ocean reanalysis is based on the NEMO model (v3.4.1) and uses the NEMOVAR data assimilation system. It assimilates a wide range of observations, including satellite altimetry and sea surface temperature, at an eddy-permitting resolution of 0.25°×0.25°.

2.2 Methods

2.2.1 Computation of the manometric component

In this study, we utilize two methods to obtain an estimate of the manometric component. One method is to use the ensemble mean of the GRACE mascon solutions from CSR, JPL, and GSFC to obtain the GRACE-based manometric estimate. The other method, an alternative to using GRACE solutions, relies on ocean reanalysis data and follows the approach developed by Camargo et al. (2023). Here, we use the sterodynamic sea level provided by the CIGAR ocean reanalysis, which combines steric ~~the global mean thermosteric~~ and dynamic sea level changes. To isolate the manometric component, we subtract the local steric effect from the sterodynamic sea level and further add the contemporary Gravitational, Rotational, and Deformation (GRD) fingerprints (representing solid Earth deformations and gravitational effects due to present-day land ice melt and terrestrial water storage changes; Gregory et al.,

2019), to obtain a manometric component comparable to GRACE. The sea level fingerprint data used in this study are based on monthly GRD fingerprint grids (~~0.5×0.5~~ 0.5°×0.5° resolution) estimated by Adhikari et al. (2019). Since this original dataset ends in 2016, we extended the time series up to 2022 using linear extrapolation, assuming that the observed trend remains constant after 2016 (see Bouih et al., 2025 for details). This reanalysis-based estimate is hereafter referred to as CIGAR manometric. Manometric sea level change generally refers to the sea level component associated with ocean mass variations ~~(i.e., excluding the steric component)~~. It is driven by water mass exchange with the continents (such as land ice melt and terrestrial water storage changes) as well as mass redistribution within the ocean, driven by ocean circulation. However, in the context of this study, we focus exclusively on the internal mass redistribution component (with the global mean ocean mass trend removed). Therefore, the 'manometric sea level' here refers solely to the redistribution by the ocean circulation, of water mass already present in the oceans, with the GRDs effect added as explained above.

2.2.2 Post processing of the data

To ensure spatial consistency across all observing systems, all gridded data sets were spatially interpolated onto a 1°×1° grid and averaged at monthly interval. A three-month moving average filter was applied to the time series. For the spatial analysis, a common mask was applied to all gridded components to exclude regions with high uncertainty. This mask covers latitudes from 66°S to 66°N, excludes inland seas, and omits coastal regions where the distance from land is less than 300 km (see Bouih et al., 2025 for details). Seasonal signals (annual and semi-annual) are removed from the time series through a least-squares adjustment of 6 and 12-month sinusoids. For the spatial maps, this least-squares fit was used to calculate the trends at each grid point. Finally, the globally averaged trend of each data set computed over the study

period was subtracted from each grid point before constructing the spatial trend maps to focus on regional spatial patterns. The study period spans from January 2004 to December 2022.

2.2.3 Data uncertainties

For the altimetry grids, we use the uncertainties estimated by Prandi et al. (2021). For the GRACE-based manometric component, uncertainties are derived from the dispersion of the data sets with respect to the ensemble mean. For the CIGAR-based manometric, thermosteric, halosteric and steric data, the dispersion of the 32 realizations around the ensemble mean was used to estimate the uncertainties. For the residual time series, the uncertainty was estimated using the law of error propagation, considering all terms of the sea level budget. Regarding the trend uncertainty, it is expressed as the standard error of the least-squares fit. To obtain the uncertainty at the 95% confidence level, we scaled the standard error by a factor of 2 (representing the 2-sigma interval).

3 Results

3.1 Comparison of the different manometric components over the North Atlantic

Figure 1~~Figure 1~~~~Figure 1~~a, b, shows the spatial manometric trend in the North Atlantic using the GRACE and CIGAR manometric data. Comparing Figure 1(a) and (b), we distinctly observe ~~distinctly~~ contrasting patterns between the GRACE and CIGAR manometric components. For the GRACE-based component, significant negative trends dominate most of the basin, with magnitudes gradually weakening from east to west. However, positive trends are observed in the western tropical Atlantic. In contrast, the CIGAR manometric component displays positive trends in the east and negative trends in the west, separated by a distinct dividing line, which likely corresponds to the position of the Mid Atlantic Ridge.

Figure 1~~Figure 1~~c also shows the 'Altimetry minus SIO-based steric 0-2000m' trends. This map is supposed to represent the manometric component, plus any deep ocean contribution.

Comparing Figure 1~~Figure 1~~c with Figure 1~~Figures 1~~a-b, we note a better agreement between 'Altimetry minus SIO' and CIGAR manometric in the Eastern Atlantic, both maps showing positive trends, while ~~unlike~~ the GRACE manometric trends are negative in this region. On the other hand, it is worth noting that the positive trend area seen in the GRACE manometric map in the western Atlantic around 30°N is also seen in the 'Altimetry minus SIO' trend map, but not in the CIGAR manometric map.

Over all, such comparisons point to problems in GRACE data in the eastern North Atlantic region.

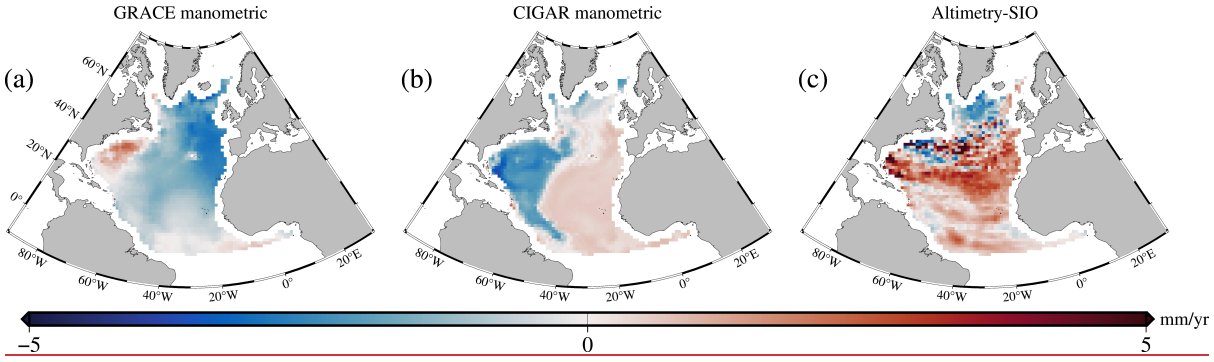

Figure 1. Manometric sea level trends in the North Atlantic over 2004.01-2022.12 derived from (a) the mean of three GRACE mascon solutions, ~~and~~ (b) the CIGAR ocean reanalysis and ~~-~~(c) 'Altimetry minus SIO-based steric sea level 0-2000m'. ~~Difference between (a) and (b).~~

3.2 Comparison of the different steric products over the North Atlantic

Figure 3~~Figure 23~~~~Figure 3~~Figure 2a-c shows the thermosteric sea level (TSL) trends over 2004-2022 over the North Atlantic for the three Argo products SIO, JAMSTEC and EN4. Similarly, Figure 3~~Figure 23~~~~Figure 3~~d-f shows the halosteric sea level (HSL) trends for the same data sets and period. As expected, due to thermohaline compensation particularly strong in the North

Atlantic (e.g., Pardaens et al., 2011; Wang et al., 2010; Wunsch et al., 2007), the two components display opposite trends. Regarding the thermosteric component (Figure 3~~Figure 23~~~~Figure 3~~a-c), while all three products display similar spatial patterns, their magnitudes vary. The JAMSTEC and EN4 products show stronger positive trends around 20°N compared to the SIO product. However, all three products indicate significant positive signals in the eastern North Atlantic. The three halosteric products share similar spatial patterns; however, the magnitude of the SIO product is notably smaller than for JAMSTEC and EN4, the latter two being very similar. This difference likely results from the SIO processing that corrects for the instrumental salinity drift reported in Argo floats since 2016, whereas the other products do~~may~~ not account for this. The mapping methods used by the different processing groups, in particular the assumed different correlation radii, may also contribute to the observed differences.

The steric sea level (SSL) trends are shown in Figure 3~~Figure 23~~~~Figure 3~~g-i. The magnitude of the total steric change is smaller than that of the thermosteric component alone. This implies that the halosteric contribution plays a significant compensatory role in the North Atlantic (consistent with previous published studies~~-~~; e.g., Bouih et al., 2025; Llovel and Hochet, 2025) ~~(e.g., Bouih et al., 2025; Llovel and Hochet, 2025)~~. Unlike in the case of the global mean, the influence of salinity changes on sea level cannot be ignored in this region.

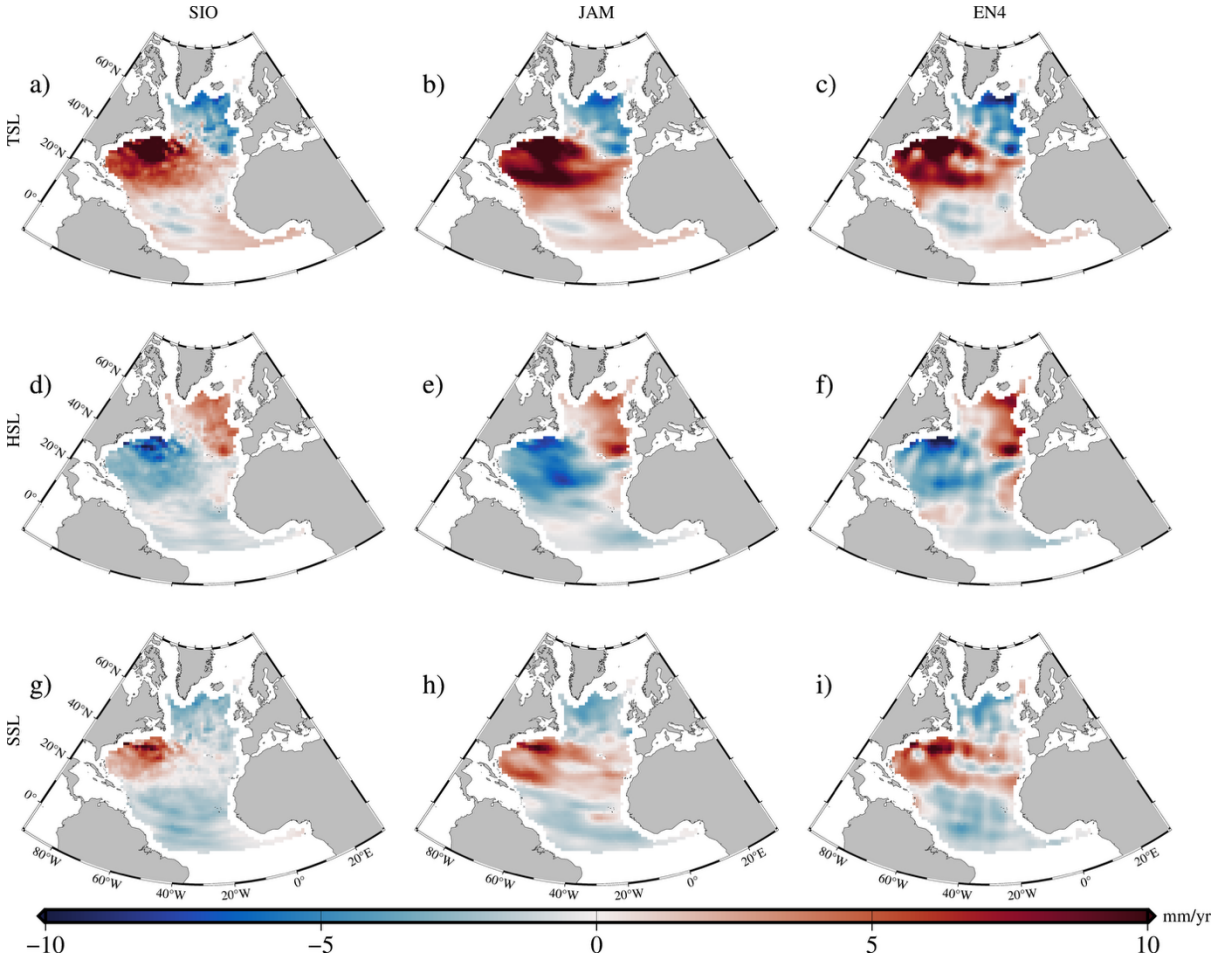

Figure 2. Trends of thermosteric (a–c), halosteric (d–f), and steric (g–i) sea level change in the North Atlantic over 2004–2022 derived from the SIO (a, d, g), JAMSTEC (b, e, h), and EN4 (c, f, i) Argo products.

3.2.1 Ocean reanalyses-based thermosteric, halosteric and steric products

In addition to Argo products, we used the CIGAR and ORAS5 ocean reanalysis data to compute thermosteric, halosteric, and steric sea level changes for both the upper 2000m and the deep

ocean (2000m-6000m), as shown in Figure 3~~Figure 3~~Figure 3~~Figure 3~~. In the upper 2000m, CIGAR and ORAS5 exhibit similar spatial patterns across all three components. Notably, the thermosteric sea level change displays a significant signal in the western North Atlantic, consistent with the Argo-based results. However, marked discrepancies between the two reanalyses are evident below 2000m. The CIGAR product displays strong positive thermosteric and negative halosteric signals in the western North Atlantic compared to ORAS5. In contrast, the deep ocean signals in ORAS5 are weak. The contrasting results of the two reanalyses for the deep ocean are puzzling and need to be investigated further. ~~. and spatially incoherent, with some areas showing even signs opposite to those observed in the upper 2000m. Consequently, the spatial patterns in CIGAR, triggered by vertical physics and, to a lesser extent, vertical error correlations embedded in the 3D-Var scheme, appear more consistent with the upper 2000m than those in ORAS5.~~

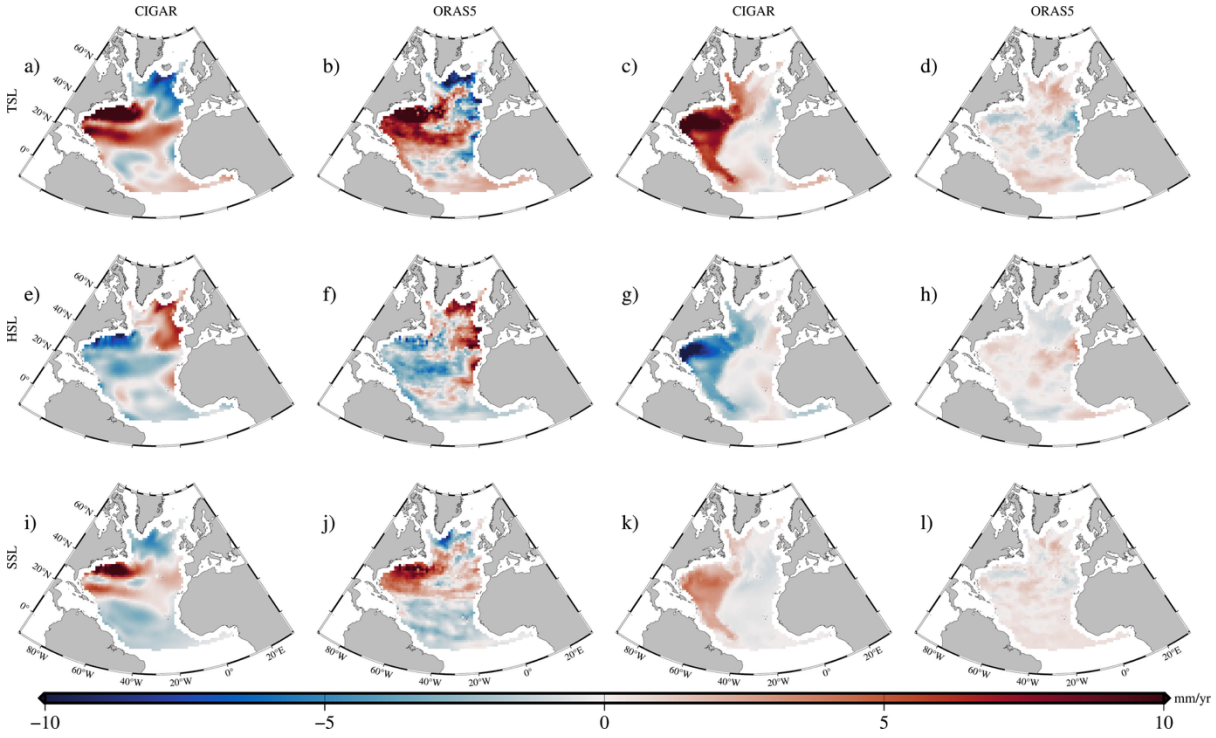

Figure 3. Trends of thermosteric (a–d), halosteric (e–h), and steric (i–l) sea level change in the North Atlantic over 2004–2022. The panels compare contributions from the upper 2000 m (a, b, e, f, i, j) and below 2000 m (c, d, g, h, k, l) derived from the CIGAR (a, c, e, g, i, k) and ORAS5 (b, d, f, h, j, l) reanalyses.

3.2.2 Argo-based and ocean reanalysis thermosteric, halosteric and steric time series

Next, we examine the thermosteric, halosteric and steric time series (weighted averages of the gridded data in the North Atlantic) for the different Argo and ocean reanalysis product (Figure ~~4Figure 4Figure 4~~). Figure ~~4Figure 4Figure 4~~a,d indicate that the thermosteric component exhibits a positive ~~an upward~~ trend in all products, although the rates of rise vary. Regarding the halosteric component (Figure ~~4Figure 4Figure 4~~b,e), we observe that the SIO and CIGAR products show a small negative ~~decreasing~~ trend that begins earlier than 2016, which may represent a true physical salinity increase during this early period. Among the three Argo

products (Figure 4~~Figure 4~~Figure 4~~Figure 4~~a-c), SIO and EN4 show strong agreement in thermosteric, halosteric, and steric sea level changes. In contrast, JAMSTEC deviates from the other two products, particularly in the halosteric component, which displays an unrealistic increase during the 2010s. Consequently, this discrepancy causes the total steric sea level change in JAMSTEC to mismatch with the other two products. In the following, we exclude the JAMSTEC product from the subsequent analysis.

Figure 4~~Figure 4~~Figure 4~~Figure 4~~d-i presents the changes for CIGAR and ORAS5 in the upper 2000m ocean depth and from 2000m to 6000m (deep ocean). In the upper 2000m, Although there is a little difference in trend before 2010, they are consistent across components after 2010, although their amplitudes slightly differ. However, in the deep ocean (2000–6000m), substantial discrepancies exist between the two products. As mentioned above, ORAS5 exhibits a weak signal in the deep ocean; its thermosteric trend is nearly zero until 2019. In contrast, CIGAR shows a consistent and distinct upward trend. Regarding the halosteric change, ORAS5 shows a small ~~weakly~~ rising trend until 2019, whereas CIGAR shows a consistent and obvious decrease. Finally, while both products exhibit rising trends in steric sea level change in the deep ocean, their magnitudes differ significantly. Given the unrealistically stationary

thermosteric signal observed in ORAS5 below 2000m, we suspect that this product is unreliable in its deep ocean variability.

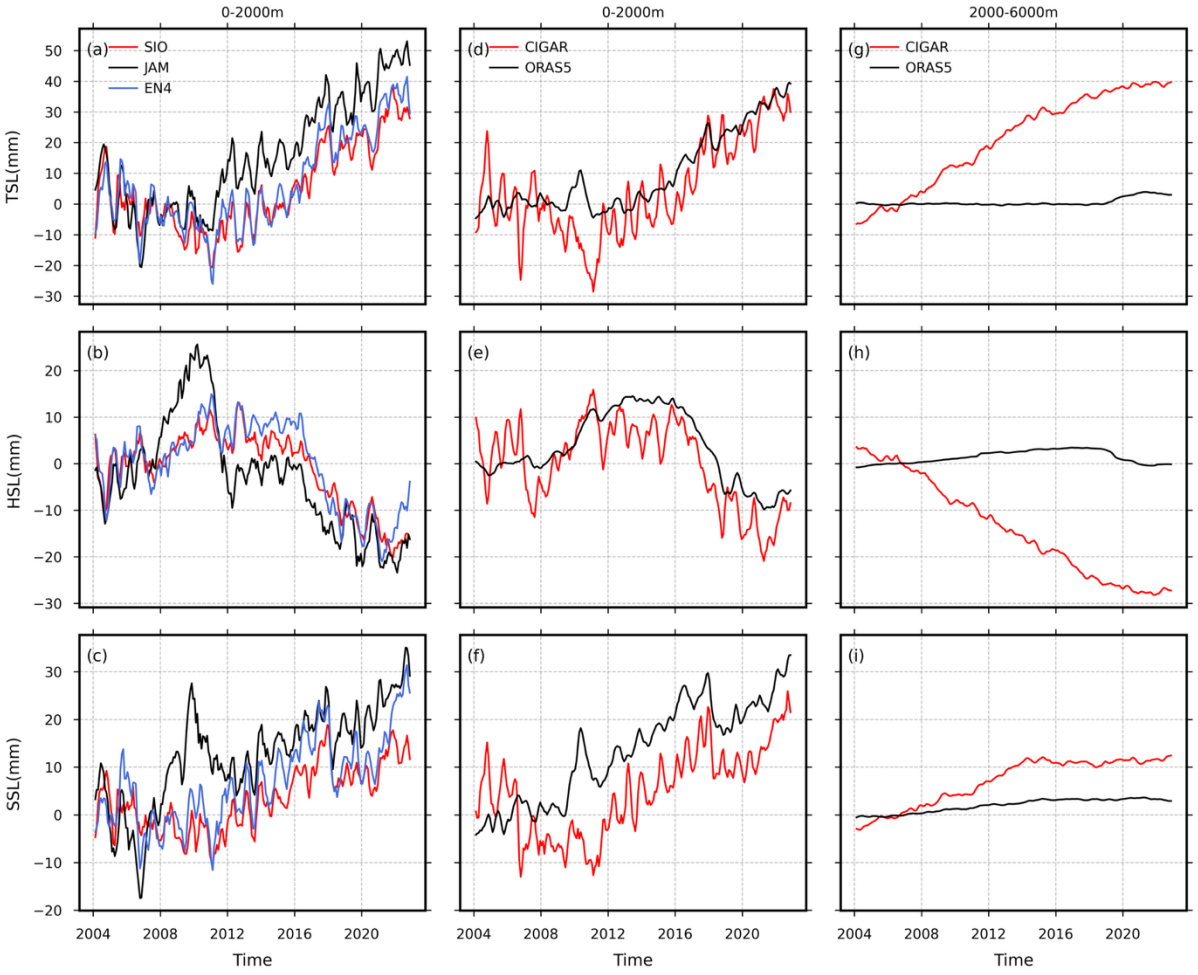

Figure 4. Time series of thermosteric (a, d, g), halosteric (b, e, h), and steric (c, f, i) sea level change in the North Atlantic. Panels (a–c) show the upper 2000 m derived from Argo products (SIO, JAM, EN4), while panels (d–i) are derived from CIGAR and ORAS5 reanalyses for the upper 2000 m (d–f) and the deep ocean 2000–6000 m (g–i). All time series have applied three-month moving average filtering. Global mean trend is included.

3.3 Comparison between the SIO steric trends and altimetry sea level trends corrected for the manometric component

In addition to directly obtaining the steric sea level trends, we can also derive it indirectly using the sea level budget equation (i.e., altimetry sea level minus manometric component computed at each grid mesh of the gridded products). In Figure 5~~Figure 5~~~~Figure 5~~, we compare the direct steric estimate from SIO with indirect estimates derived by subtracting different manometric products (GRACE or CIGAR) from altimetry ~~trend~~ data. It is important to note that the indirect method inherently includes deep ocean contribution and relies on independent observations. From Figure 5~~Figure 5~~~~Figure 5~~, we clearly observe that the spatial trend pattern of SIO is more consistent with the "Altimetry minus CIGAR manometric" estimate, as both exhibit positive signals in the western North Atlantic. In contrast, the "Altimetry minus GRACE manometric" estimate displays a prominent positive signal in the eastern North Atlantic which is absent in the SIO data. This suggests that the GRACE manometric data contains substantial inaccuracies, particularly in the eastern North Atlantic, while "Altimetry minus CIGAR manometric" agrees rather well with the SIO steric trends. Such a result confirms previous finding based on the comparison between GRACE manometric trends and 'Altimetry minus SIO-based steric' trends that already highlighted potential errors in GRACE data in the eastern North Atlantic (section 3.1).

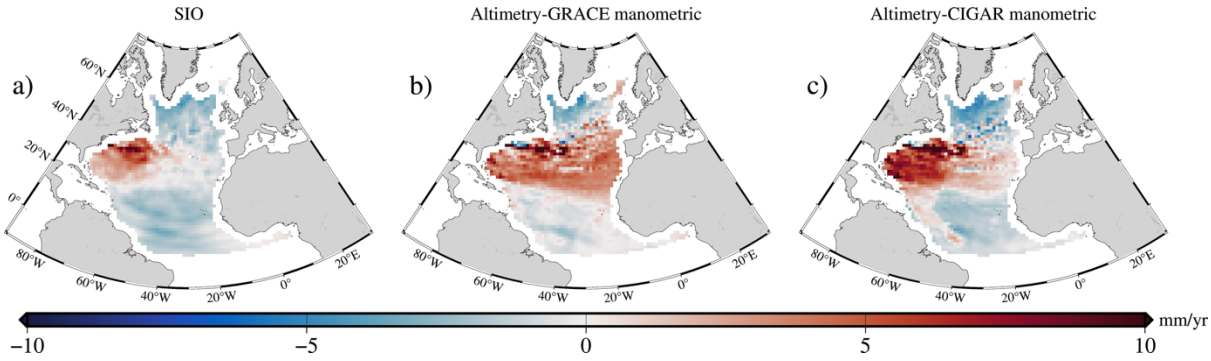

Figure 5. Steric sea level trends derived directly from SIO and indirectly from Altimetry minus manometric estimates (GRACE or CIGAR).

To highlight this further, Figure 6~~Figure 6~~~~Figure 6~~a, b shows the scatter plots between SIO gridpoint steric trends and "Altimetry minus GRACE manometric" and "Altimetry minus CIGAR manometric" grid point trends. The data have been normalized.

The scatter plots reveal distinct differences in the correlation between SIO observations and Altimetry minus ~~the~~ the two manometric estimates. In the negative SIO region (corresponding to the lower half of Figure 6~~Figure 6~~~~Figure 6~~ and the negative value~~s~~ regions in Figure 5~~Figure 5~~~~Figure 5~~), where ~~most points~~most points align with the diagonal in both cases, the ~~"~~"Altimetry-CIGAR manometric"~~"~~ estimates points are clustered notably more tightly than those in the ~~"~~"Altimetry-GRACE manometric"~~"~~ comparison. This indicates that in regions with negative steric sea level change, where both estimates correlate with SIO, the "Altimetry-CIGAR manometric" estimate maintains a higher spatial correlation compared to "Altimetry-GRACE manometric". ~~Notably, T~~the abundance of data points in the quadrant characterized by negative SIO and positive 'Altimetry-GRACE manometric' values ~~particularly~~ reflects the situation eastern ~~of the~~ North Atlantic (Figure 5), where negative SIO observations are paired with positive "Altimetry-GRACE manometric" estimates. In the positive SIO areas (corresponding to the upper half of the plots), a portion of the data points in both estimates fall below the 1:1 correspondence line ~~exhibit values lower than the SIO observations~~ (indicated

by points falling above the diagonal). However, this deviation~~underestimation~~ is much more pronounced for "~~-~~Altimetry-GRACE manometric"~~-~~, leading to a larger spread away from the diagonal compared to "Altimetry-CIGAR manometric". This suggests that while the linear consistency ~~correlation~~ with SIO decreases for both products in positive steric sea level trend regions (such as the western North Atlantic), the correlation of "Altimetry-GRACE manometric" is notably weaker than that of "Altimetry-CIGAR manometric".

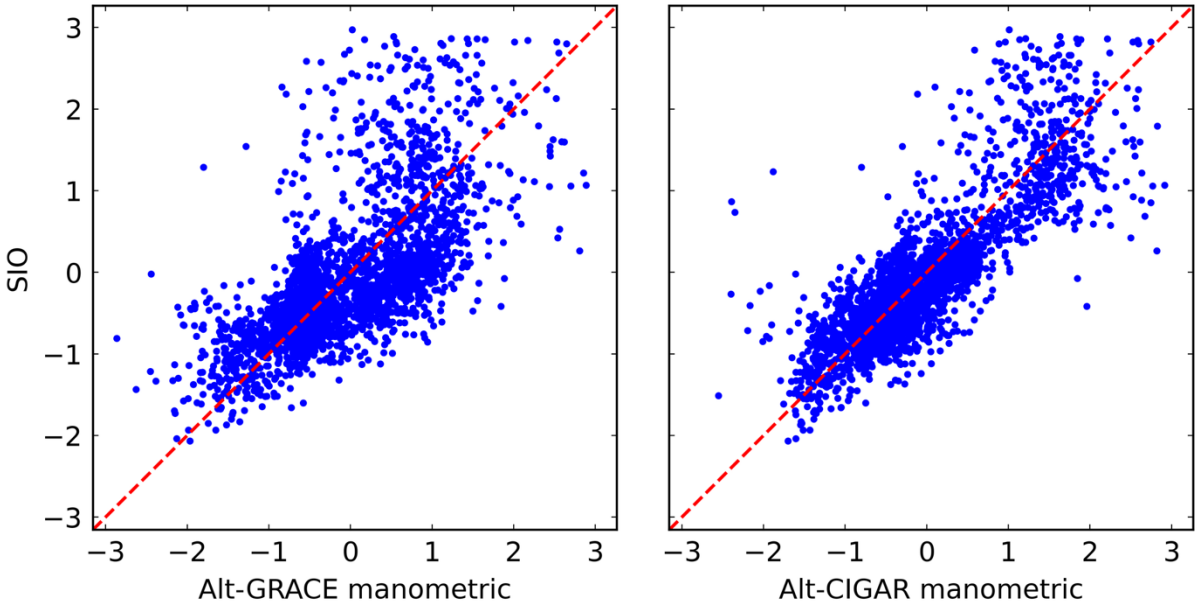

Figure 6. Scatter plots of SIO steric sea level change versus Altimetry minus manometric estimates (GRACE/left or CIGAR/right). The data have been normalized and outliers exceeding 3σ were removed.

3.4 Residual trend maps in the North Atlantic

In this section, we utilize data from the observing systems described above to compute spatial maps of the sea level budget residuals.

3.4.1 North Atlantic budget residuals for~~of~~ different manometric and steric (0-2000m) components

We computed the residuals by subtracting various combinations of manometric (GRACE, CIGAR) and steric (SIO, EN4, CIGAR, and ORAS5 upper 2000 m) components from the altimetry data (Figure 7).

As shown in Figure 7a,e, the resulting residuals implicitly include a deep ocean steric contribution, which is not accounted for since the steric data are limited here to the upper 2000 m. This is consistent with previous results from Bouih et al. (2025), who observed positive residuals in the North Atlantic for both manometric cases., Similarly positive residuals are found in the eastern North Atlantic for the GRACE manometric component and in the western North Atlantic for the CIGAR manometric component.

From Figure 7, we also observe that the spatial distribution of the residuals remains similar when the manometric component is held fixed while varying the steric components. However, the residual magnitude is different. Specifically, when using the GRACE manometric component, the positive signal derived from SIO is stronger in the eastern North Atlantic compared to other steric products. When using the CIGAR manometric component, the positive signals from SIO and CIGAR are stronger in the western North Atlantic compared to EN4 and ORAS5.

To quantify the residuals, we computed the latitude-weighted spatial mean trend of each map. Results are shown in Table 1~~Table 1~~~~Table 1~~ (remind that results in Table 1~~Table 1~~~~Table 1~~ do not account for the global mean trends). From Table 1~~Table 1~~~~Table 1~~, we observe that regardless of the steric data used (whether from Argo or ocean reanalyses), the residuals derived using the CIGAR manometric component are always smaller than those derived using GRACE. Furthermore, for a given manometric component, the residual with SIO is larger than

that with EN4, even though SIO has corrected for the salinity drift since 2016. Besides, the residual with CIGAR steric is larger than that with ORAS5.

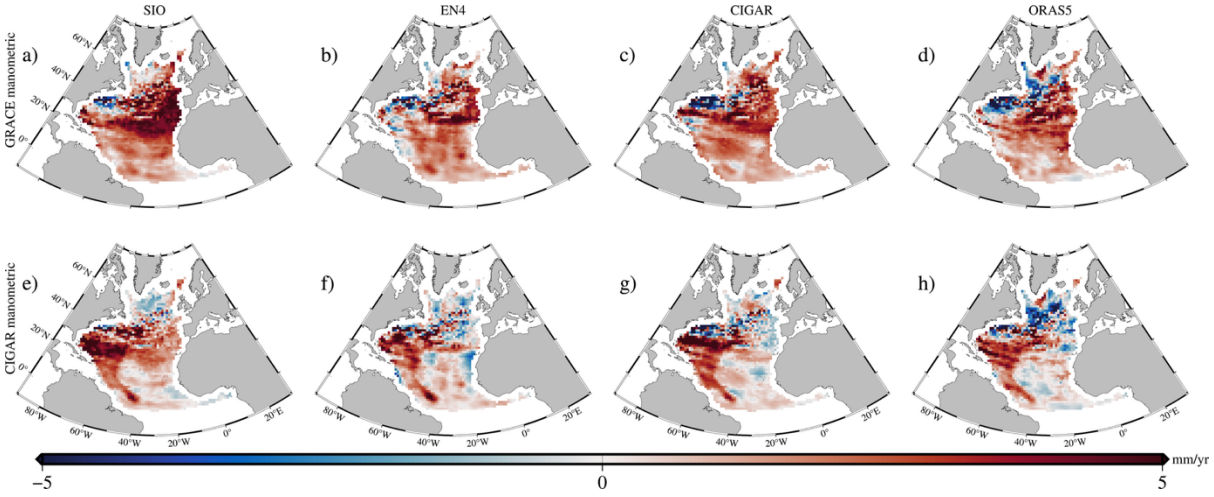

Figure 7. Maps of sea level residuals (mm/yr) in the North Atlantic. The residuals are calculated by subtracting manometric and steric components from satellite altimetry. The manometric component is derived from GRACE (a–d) and CIGAR (e–h). These are combined with upper 2000 m steric estimates from SIO (a, e), EN4 (b, f), CIGAR (c, g), and ORAS5 (d, h).

Table 1. Trend values (mm/yr) of sea level residuals in the North Atlantic corresponding to different steric products (0-2000m) and the two manometric components. Global mean trends were removed. Uncertainties are 2-sigma errors of the least-squares fit.

Trend (mm/yr)	SIO	EN4	CIGAR	ORAS5
GRACE manometric	2.15±0.19	1.43±0.22	1.52±0.21	1.10±0.20
CIGAR manometric	1.50±0.23	0.77±0.23	0.86±0.25	0.45±0.16

3.4.2 North Atlantic budget residuals and deep ocean steric contribution

In this section, we added the deep ocean steric sea level change to the upper 2000 m steric estimates, considering both the CIGAR and ORAS5 deep steric data, and using either GRACE or CIGAR for the manometric components. Resulting residual trends are shown in Figure 8~~Figure 8~~~~Figure 8~~ . For all cases except the ORAS5 deep ocean case, ~~-~~the residuals derived using GRACE manometric data (Figure 8~~Figure 8~~~~Figure 8~~a–c) show a dipole pattern (positive in the east, negative in the west) compared to the results without the deep ocean component (Figure 7). Table 2~~Table 2~~~~Table 2~~ summarizes the residual trend values for all cases (as for Table 1~~Table 1~~~~Table 1~~, remind that results in Table 2~~Table 2~~~~Table 2~~ do not account for the global mean trends). Comparing results from Table 1~~Table 1~~~~Table 1~~ and Table 2~~Table 2~~~~Table 2~~, we note that the mean residual magnitude is significantly reduced when the deep ocean steric change is included: by ~30% when using GRACE for the manometric component and SIO for the upper 0-2000m steric sea level, and by ~50% when using CIGAR for both the steric (full depth and manometric component). Based on CIGAR, the deep steric contribution to the North Atlantic sea level budget (in addition to the global mean deep ocean contribution) amounts to 0.62 ± 0.04 mm/yr.

In contrast, when using the CIGAR manometric component (Figure 8~~Figure 8~~~~Figure 8~~e–h), the residuals decrease significantly in both spatial variability and magnitude. Notably, the sea level budget is effectively nearly closed within error bars when combining CIGAR manometric and CIGAR steric data. Finally, it is worth noting that for SIO, positive residuals are observed in the eastern North Atlantic regardless of whether GRACE or CIGAR manometric data is used.

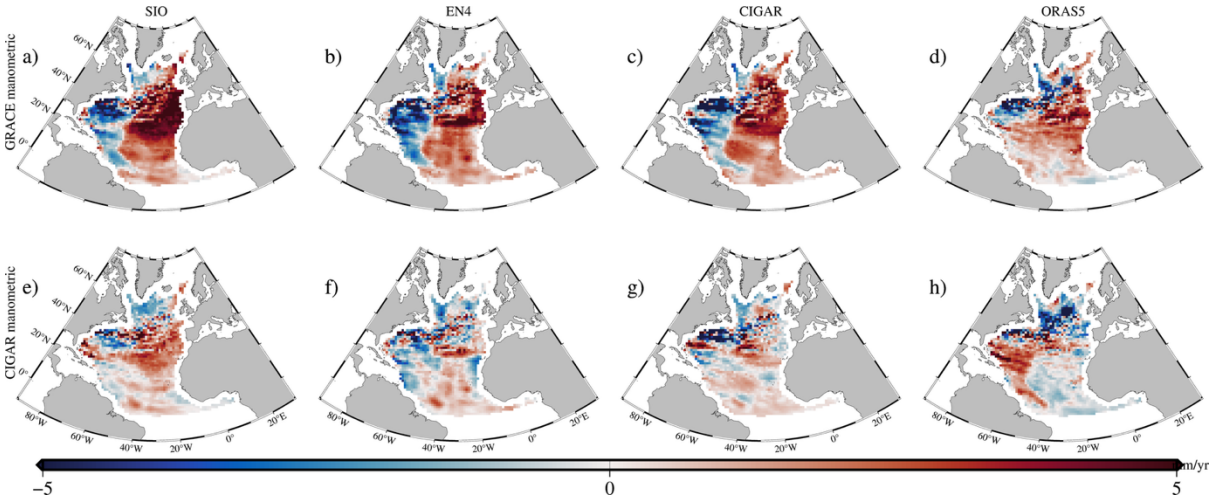

Figure 8. Maps of sea level residuals (mm/yr) in the North Atlantic, calculated as in Figure 7 but with the inclusion of the deep ocean (below 2000 m) steric component. The deep ocean contribution is derived from CIGAR for panels (a–c, e–g) and from ORAS5 for panels (d, h). In panels a-c, the manometric component is from GRACE while it is from CIGAR in panels e-h.

Table 2. Trend values (mm/yr) over 2004-2022 of sea level residuals in the North Atlantic for four steric products and two manometric components, accounting for the deep ocean. For SIO and EN4, the deep ocean contribution from CIGAR is added. For CIGAR and ORAS5, their own deep steric contributions are considered. Global mean trends removed. Uncertainties are 2-sigma errors of the least-squares fit.

Trend (mm/yr)	SIO + CIGAR Deep ocean	EN4 + CIGAR Deep ocean	CIGAR Full depth	ORAS5 Full depth
GRACE manometric	1.53±0.21	0.81±0.24	0.90±0.23	0.87±0.20
CIGAR manometric	0.88±0.20	0.15±0.21	0.24±0.22	0.22±0.15

3.5 Time series of the North Atlantic mean sea level budget

Based on the analysis above, the deep ocean contribution to the North Atlantic sea level budget cannot be ignored. To assess the influence of the deep ocean on the sea level budget, we computed time series for each component, including total sea level, manometric sea level, thermosteric sea level, and halosteric sea level. Compared to results discussed above, here we account for the global mean trend of each component.

3.5.1 North Atlantic mean sea level budget time series without deep ocean (global mean trends included)

Here, we have reintroduced the global mean trend of each component. Since the CIGAR manometric component does not fully account for the external sea water mass addition to the ocean due to land ice melt and terrestrial waters, we adopt GRACE data to represent the total ocean mass ~~manometric sea level~~ change (i.e., global mean trend accounted for). Regarding the steric sea level component, we selected the SIO product for Argo estimates, as it corrects for the salinity drift. For ocean reanalyses, we only consider the CIGAR reanalysis.

Figure 9~~Figure 9~~~~Figure 9~~ presents the sea level budget time series (global mean trends accounted for) in the North Atlantic without the deep ocean steric sea level change. Residual time series are also shown. The left/right panels use SIO/CIGAR steric sea level change in upper 2000m. Comparing Figure 9~~Figure 9~~~~Figure 9~~ left and right panels, we observe that the halosteric components from SIO and CIGAR slightly differ. For SIO, a slight halosteric decrease is observed over 2012-2015, with a linear trend of -1.10±0.94 mm/yr during the such period, then it increases to -3.20±0.9 mm/yr over 2016-2022. Consequently, the SIO halosteric trend over 2012-2022 amounts to -2.87±0.21 mm/yr. In terms of global mean trend, the SIO halosteric time series does not show any trend (as expected since the salinity drift is supposed to be corrected). Thus, the SIO halosteric decrease observed in the North Atlantic may possibly reflect a tru~~ly~~ physical salinity increase. As of 2016, the CIGAR halosteric decrease is slightly

larger than for SIO, possibly a consequence of the salinity drift error not corrected for in the assimilated EN4 salinity data. The mean residual trends amount to 2.72±0.19 mm/yr and 2.34±0.21 mm/yr for the SIO and CIGAR steric cases respectively, i.e., not significantly different. Results are gathered in Table 3.

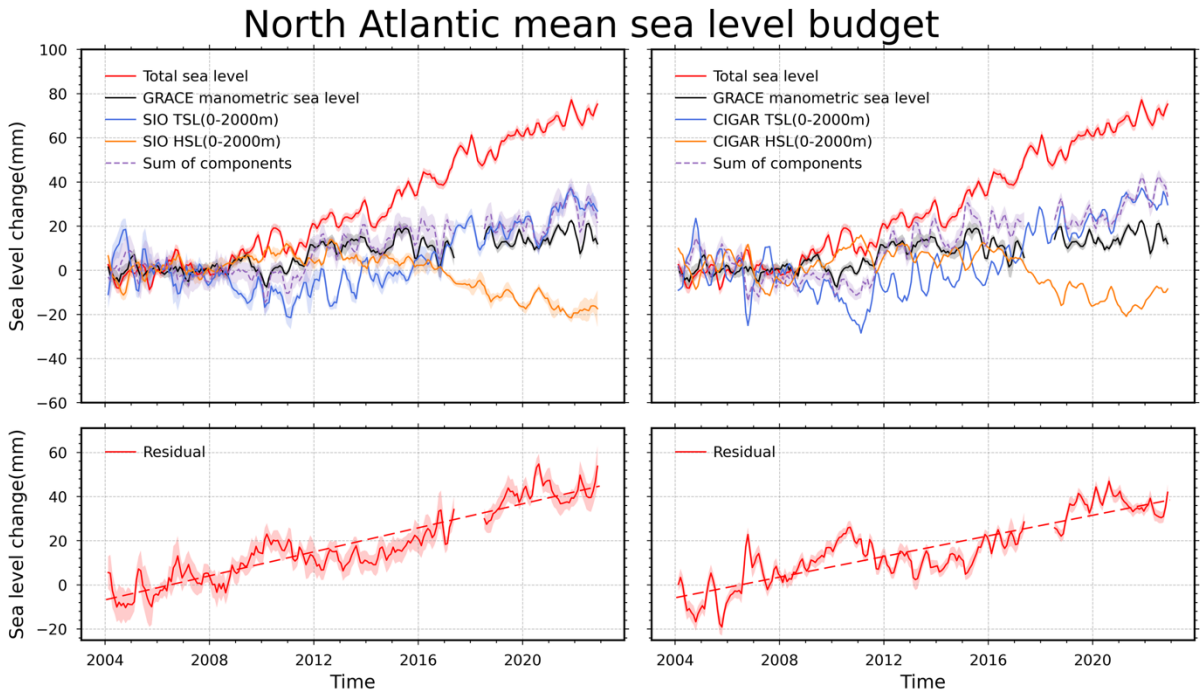

Figure 9. Time series of North Atlantic sea level components (top) and residuals (bottom) for the upper 2000m. The analysis uses Altimetry and GRACE ~~manometric~~ data, combined with steric estimates from SIO (left) and CIGAR (right). All time series have applied three-month moving average filtering. The global mean trend of each component is included.

Table 3. Components of the North Atlantic sea level budget over 2004-2022 (upper ocean 0-2000m, Global mean trends included)

Components of the North Atlantic	**Linear trends (mm/yr)**
Altimetry	4.45±0.16
GRACE ocean mass	1.03±0.13
Thermosteric SIO (0-2000m)/CIGAR (0-2000m)	1.76±0.27/1.92±0.29
Halosteric SIO (0-2000m)/CIGAR (0-2000m)	-1.01±0.17/-0.8±0.19
Sum of steric and mass components SIO (0-2000m)/CIGAR (0-2000m)	1.73±0.19/2.11±0.22
Residuals SIO (0-2000m)/CIGAR (0-2000m)	2.72±0.19/2.34±0.21

3.5.2 North Atlantic sea level budget time series with the deep ocean contribution (global mean trends included)

In this section, we add the deep ocean contribution from the CIGAR reanalysis. As in section 3.5.1, the GRACE-based ocean mass ~~manometric~~ component is considered, and for the upper 2000m steric component, both SIO and CIGAR data are used. The corresponding sea level budget time series for the North Atlantic are shown in Figure 10.

As illustrated in Figure 10, with the inclusion of the deep ocean contribution, the halosteric decline in both panels become more evident compared to the case without the deep ocean. Specifically, the CIGAR component also shows a slight decrease starting in 2012. However, unlike the SIO trend, which maintains a relatively stable decline throughout the study time span, the CIGAR decrease still exhibits a sudden intensification after 2016. Similarly, the thermosteric sea level also displays a stronger positive~~increasing~~ trend compared to the case without the deep ocean.

Consequently, the total steric sea level trend is larger than in the case without the deep ocean contribution. Finally, the inclusion of the deep ocean contribution leads to a reduction in the North Atlantic residual trends for both cases: for the estimate based on SIO (upper 2000 m), the trend decreases by about 30%, from 2.72±0.19 mm/yr to 1.89±0.21 mm/yr, whereas for the estimate based on CIGAR, it drops from 2.34 ± 0.21 mm/yr to 1.51 ± 0.23 mm/yr. Corresponding results are presented in Table 4.

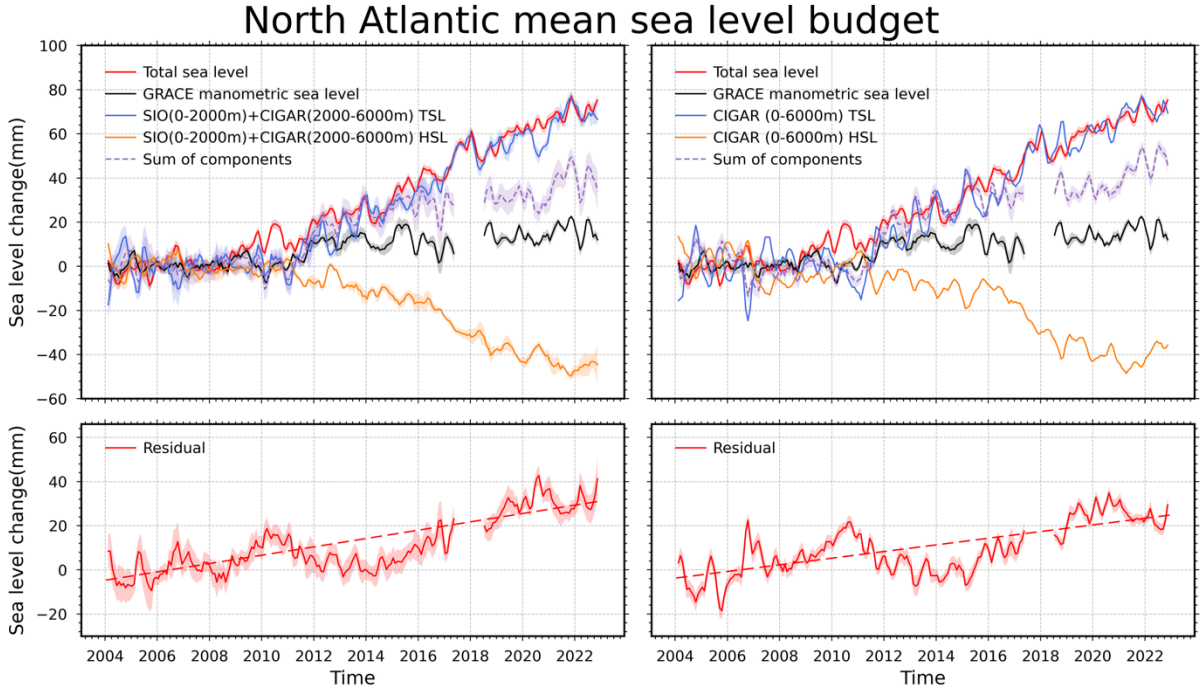

Figure 10. Time series of North Atlantic sea level change components (top) and budget residuals (bottom). The left panels use a hybrid steric estimate (SIO for 0–2000m combined with CIGAR for 2000–6000m), while the right panels use the full-depth CIGAR steric estimate (0–6000m). In both cases, Altimetry and GRACE ~~manometric~~ data are used. All time series have applied three-month moving average filtering. The global mean trend of each component is included.

Table 4. Components of the North Atlantic sea level budget over 2004-2022 (full depth 0-6000m, Global mean trends included)

Components of the North Atlantic	Linear trends (mm/yr)
Altimetry	4.45 ±0.16
GRACE ocean mass	1.03±0.13
Thermosteric SIO (0-2000m) + CIGAR (2000-6000m)/CIGAR Full depth	4.47±0.24/4.64±0.27
Halosteric SIO (0-2000m) + CIGAR (2000-6000m)/CIGAR Full depth	-2.9±0.16/-2.68±0.19
Sum of steric and mass components (with SIO 0-2000m + CIGAR 2000-6000m)/CIGAR Full depth	2.56±0.19/2.94±0.22
Residuals (with SIO 0-2000m + CIGAR 2000-6000m)/CIGAR Full depth	1.89±0.21/1.51±0.23

3.5.3 Sea level budget of all oceans but without the North Atlantic Ocean, with the deep ocean contribution added (global mean trends included).

In (Bouih et al. (, 2025)'s study, the sea level budget for the global ocean excluding the North Atlantic (without the deep ocean steric contribution) was not closed. In this section, we consider the deep ocean steric sea level change contribution to the sea level budget. We compute the sea level budget for the global ocean excluding the North Atlantic using the same data products as in Section 3.5.2. The corresponding results are shown in Figure 11.

In the left panel (using SIO data for the upper 2000 m), we observe that the halosteric sea level change is nearly zero. The residual is very small, estimated at 0.16±0.08 mm/yr. Thus,

considering the whole oceanic domain without the North Atlantic, the sea level budget is closed when SIO data are used for the upper 2000 m ocean layer. In contrast, the right panel (using CIGAR data for all depths) shows a distinct decrease in halosteric sea level starting in 2016, due to the assimilation of EN4 data in CIGAR (not corrected for the salinity drift). Nevertheless, the residual trend of the right panel is small (0.51±0.11 mm/yr), suggesting quasi closure of the sea level budget.

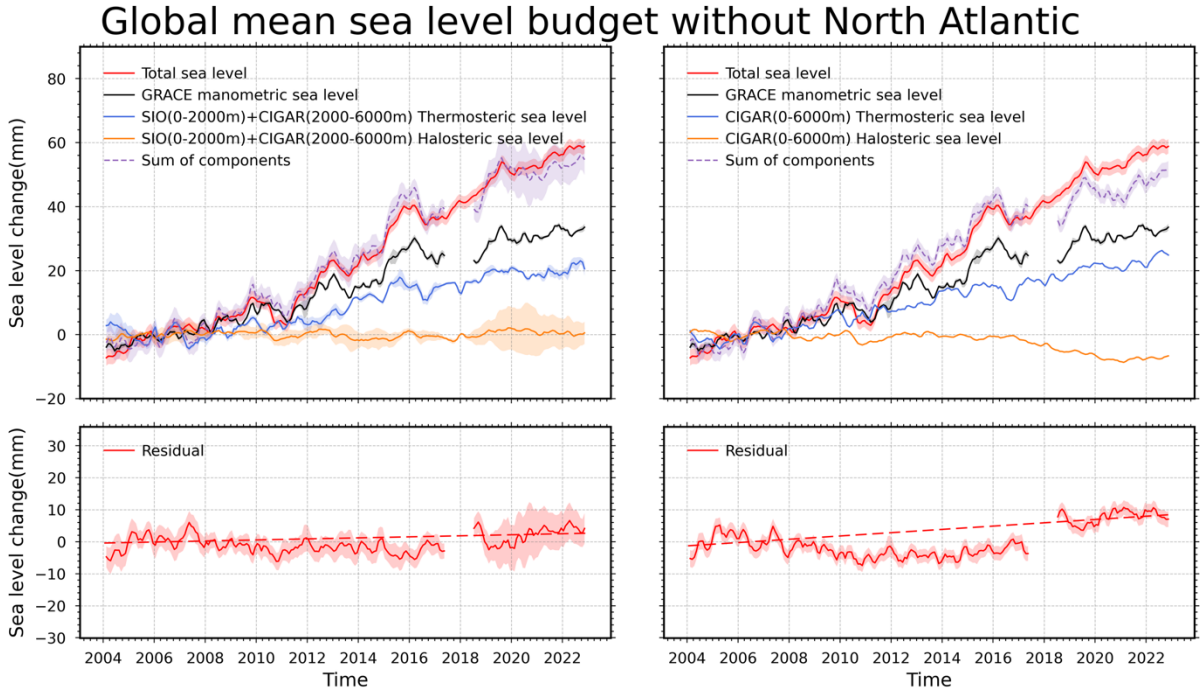

Figure 11. Time series of sea level components (top) and residuals (bottom) for the global ocean excluding the North Atlantic. The left panels use a hybrid steric estimate (SIO for 0–2000 m combined with CIGAR for 2000–6000m), while the right panels use the full-depth CIGAR estimate (0–6000m). All time series have applied three-month moving average filtering. The global mean trend of each component is included.

552 *3.5.4 North Atlantic sea level budget time series with the deep ocean contribution (global mean*
553 *trends removed)*

554 Here, we compute the North Atlantic sea level budget (including the deep ocean contribution)
555 with the global mean sea level trends of all components removed. The objective is to determine
556 which part of the non-closure in the North Atlantic budget may result from errors in the regional
557 components (i.e., independently from errors in the global mean trends). Figure 12 presents the
558 budget time series using GRACE for the manometric component. We consider two steric cases:
559 the hybrid case (SIO 0–2000 m plus CIGAR deep ocean) and the CIGAR full-depth case.
560 The mean residual trends are estimated at 1.53 ± 0.21 mm/yr for the hybrid steric case and
561 0.88 ± 0.20 mm/yr for the CIGAR full-depth case. Comparing these results (where global mean
562 trends are removed) with those in Figure 10 (where global mean trends are included), we
563 observe very little difference in the mean residual trends. This suggests that errors in the global
564 mean trends are small, and that the reported residuals in the North Atlantic budget are primarily
565 driven by component errors at the regional scale.
566

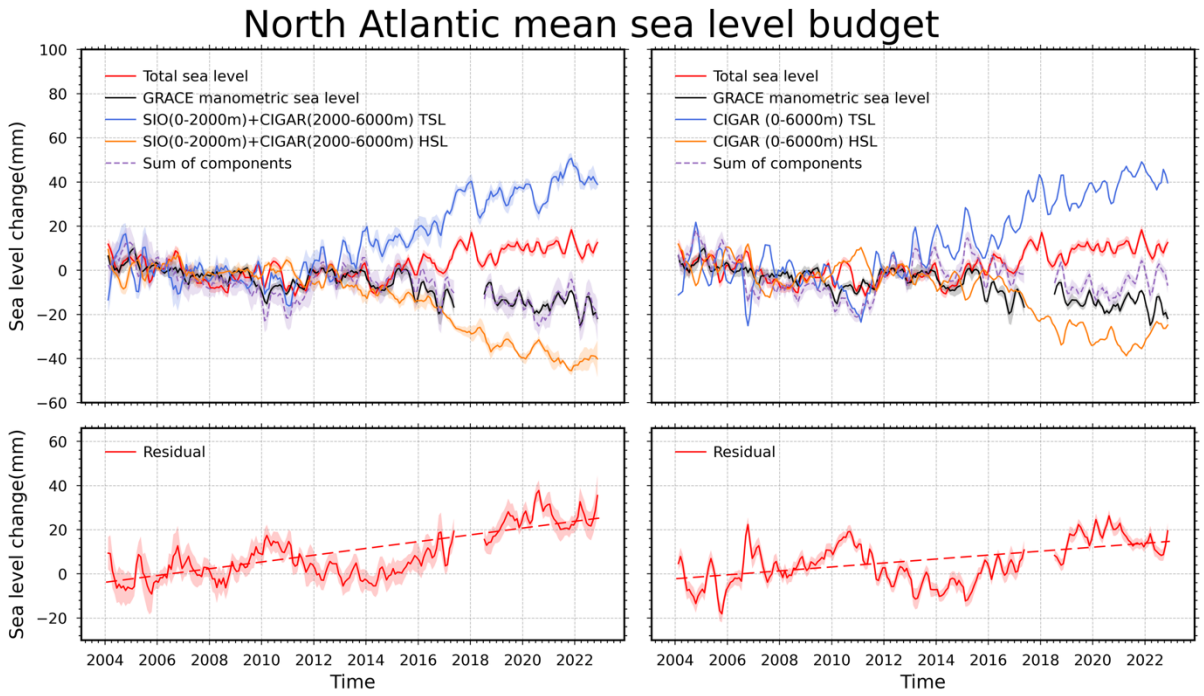

Figure 12. Time series of North Atlantic sea level change components (top) and budget residuals (bottom). The left panels use a hybrid steric estimate (SIO for 0–2000m combined with CIGAR for 2000–6000m), while the right panels use the full-depth CIGAR steric estimate (0–6000m). In both left and right panels, GRACE manometric components are considered. All time series have applied three-month moving average filtering. The global mean trend of each component is removed.

Figure 13 displays the corresponding budget time series using CIGAR for the manometric component. Similarly, we evaluate the residuals for both steric configurations. When using the CIGAR manometric data, the mean residual trends amount to 0.88±0.20 mm/yr for the hybrid steric case (SIO 0–2000 m plus CIGAR deep ocean) and 0.24±0.22 mm/yr for the CIGAR full-depth case.

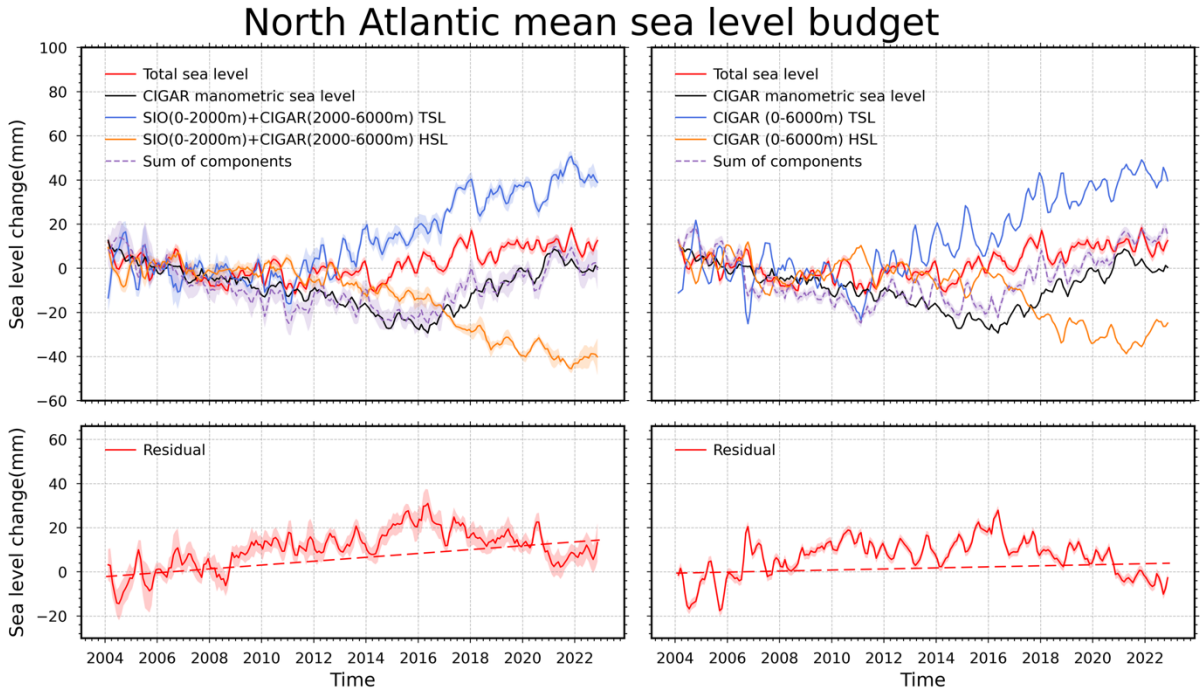

Figure 13. Time series of North Atlantic sea level change components (top) and budget residuals (bottom). The left panels use a hybrid steric estimate (SIO for 0–2000m combined with CIGAR for 2000–6000m), while the right panels use the full-depth CIGAR steric estimate (0–6000m). In both left and right panels, CIGAR manometric components are considered. All time series have applied three-month moving average filtering. The global mean trend of each component is removed.

Comparing the results from Figure 12 and Figure 13, we note that using CIGAR for the manometric component consistently leads to smaller regional residuals than using GRACE, regardless of the steric product considered. It is worth noting that the configuration using CIGAR for both manometric and steric components yields a mean residual trend of 0.24±0.22 mm/yr, nearly four times smaller than in the case where the GRACE manometric component is used (0.90±0.23 mm/yr). These results confirm our previous conclusions based on the residual trend maps. The trends of the residual time series for the different products of the sea

level budget (global mean trends removed) are identical to those presented in Table 2 (gridded averages) and are not reproduced here.

4 Discussion

In this study, we have revisited the sea level budget of the North Atlantic over the 2004-2022 period, using a variety of different data sets. The objective was to further investigate the results from Bouih et al. (2025) who reported non-closure of the sea level budget in the North Atlantic over the same time span, and to identify which components of the budget (or which missing component) are responsible.

The main results of our study can be summarized as follows:

(1) By comparing the GRACE and CIGAR manometric trends with the 'Altimetry minus steric sea level', we note a better agreement (same positive sign) between the latter and the CIGAR-based manometric component in the northeastern Atlantic, while the GRACE manometric trends have an opposite (negative) sign in this region.

~~(1)~~ (2) By comparing the SIO-based steric sea level trends with "Altimetry minus manometric sea level" in two cases (GRACE and CIGAR-based manometric component) over the North Atlantic, the use of CIGAR manometric sea level provides higher correlation than when using GRACE. This comparison together with the one presented in (1) indicates potential errors in the GRACE and GRACE-FO data, particularly in the eastern region of the North Atlantic basin where the manometric component is strongly negative. The cause is so far unknown but possibly related to the correction applied to GRACE data, e.g., the geocenter or GIA corrections. These needs dedicated investigation.

~~(2)~~ (3) As of 2012, a ~~decreasing~~negative trend is observed in the SIO halosteric component which suggests a physically real increase in salinity of the North Atlantic. Again, this needs further investigation.

~~(3)~~ (4) Our study shows that the deep ocean (>2000 m of depth) contribution to the North Atlantic sea level budget is not negligible and needs to be taken into account to obtain better closure of the sea level budget in this region. Based on CIGAR, the additional deep ocean steric contribution (above the global mean deep ocean contribution) to the North Atlantic sea level budget amounts to 0.62 ± 0.04 mm/yr.

~~(4)~~ (5) Accounting for the deep ocean steric contribution reduces by a factor of 30% the residuals of the North Atlantic sea level budget when using the GRACE manometric component, and by a factor of 50% ~~two~~ when using CIGAR for the manometric component (and CIGAR full depth for the steric component). In the latter case, the mean residual trend over the North Atlantic is <1mm/yr, i.e., of the same order of magnitude as the regional trend error for altimetry gridded data according to Prandi et al. (2021). We can thus conclude that the closure of the sea level budget holds within the data uncertainties in this case.

~~(5)~~ (6) Our results also indicate that the main contribution to the mean North Atlantic residual trend comes from errors on the regional components (whatever the products used for the components) rather than from errors in the global mean trends.

~~(6)~~ (7) The North Atlantic sea level budget is closed within data uncertainties when using the CIGAR reanalysis for both the manometric and steric components.

~~(7)~~ (8) Our study also shows that the sea level budget of all other oceans (North Atlantic excluded) is almost closed when accounting for the deep ocean steric contribution based on the CIGAR ocean reanalysis

To conclude, t~~T~~hese new findings represent a step further towards better understanding of the present-day sea level budget in the North Atlantic region. Th~~co~~se investigations also support the need to better observe the deep ocean especially in the North Atlantic Ocean which is one of the objectives of the One Argo Project (Thierry et al., 2025). Nevertheless, some issues still merit deeper investigation. We can quote the followings, among others: Why GRACE manometric data give less good results in the Northeast Atlantic than the CIGAR-based manometric sea level? Which inaccurate correction applied to GRACE is involved? Is it related to the GIA or the geocenter corrections applied to GRACE? What causes the slight salinity increase observed in the North Atlantic (full depth) with SIO data? Can we explain the physical process causing the reported CIGAR-based positive deep ocean steric sea level? What is the impact on the CIGAR steric component estimates of the use of EN4 (with no salinity drift correction applied) in the assimilation procedure? What is the source of the (small) remaining residual trend of the North Atlantic sea level budget (after accounting for the deep ocean)? Clearly, future studies should be devoted to try answering these puzzling questions.

Author contributions

AC, WL and ZS designed the study. All analyses have been performed by ZS. ZS and AC wrote a first version of the manuscript. All co-authors contributed to the discussion of the results, editing and final writing of the manuscript.

Competing interests

The contact author has declared that none of the authors has any competing interests.

Acknowledgements

The authors thank two anonymous reviewers for helpful comments that significantly improved the manuscript. Zhe Song is supported by China Scholarship Council. This study is a contribution to the ongoing ESA (European Space Agency) CCI (Climate Change Initiative) project entitled 'Sea level budget closure CCI+ (SLBC_CCI+)'. This work is a contribution to the GREAT project funded by CNES through the Ocean Surface Topography Science Team (OSTST).

675 **References**

676 Adhikari, S., Ivins, E. R., Frederikse, T., Landerer, F. W., and Caron, L.: Sea-level fingerprints
677 emergent from GRACE mission data, Earth System Science Data, 11, 629–646,
678 https://doi.org/10.5194/essd-11-629-2019, 2019.
679 Barnoud, A., Pfeffer, J., Guérou, A., Frery, M., Siméon, M., Cazenave, A., Chen, J., Llovel,
680 W., Thierry, V., Legeais, J., and Ablain, M.: Contributions of Altimetry and Argo to Non-
681 Closure of the Global Mean Sea Level Budget Since 2016, Geophysical Research Letters, 48,
682 https://doi.org/10.1029/2021gl092824, 2021.
683 Bouih, M., Barnoud, A., Yang, C., Storto, A., Blazquez, A., Llovel, W., Fraudeau, R., and
684 Cazenave, A.: Regional sea level trend budget over 2004–2022, Ocean Sci., 21, 1425–1440,
685 https://doi.org/10.5194/os-21-1425-2025, 2025.
686 Brown, S., Willis, J., and Fournier, S.: Jason-3 Wet Path Delay Correction,
687 https://doi.org/10.5067/J3L2G-PDCOR, 2023.
688 Camargo, C. M. L., Riva, R. E. M., Hermans, T. H. J., Schütt, E. M., Marcos, M., Hernandez-
689 Carrasco, I., and Slangen, A. B. A.: Regionalizing the sea-level budget with machine learning
690 techniques, Ocean Science, 19, 17–41, https://doi.org/10.5194/os-19-17-2023, 2023.
691 Chen, J., Tapley, B., Seo, K., Wilson, C., and Ries, J.: Improved Quantification of Global Mean
692 Ocean Mass Change Using GRACE Satellite Gravimetry Measurements, Geophys. Res. Lett.,
693 46, 13984–13991, https://doi.org/10.1029/2019GL085519, 2019.
694 Chen, J., Tapley, B., Wilson, C., Cazenave, A., Seo, K.-W., and Kim, J.-S.: Global Ocean Mass
695 Change From GRACE and GRACE Follow-On and Altimeter and Argo Measurements,
696 Geophysical Research Letters, 47, e2020GL090656, https://doi.org/10.1029/2020GL090656,
697 2020.
698 Cheng, L., Zhu, J., Cowley, R., Boyer, T., and Wijffels, S.: Time, Probe Type, and Temperature
699 Variable Bias Corrections to Historical Expendable Bathythermograph Observations, Journal

of Atmospheric and Oceanic Technology, 31, 1793–1825, https://doi.org/10.1175/JTECH-D-13-00197.1, 2014.

Dieng, H. B., Cazenave, A., Meyssignac, B., and Ablain, M.: New estimate of the current rate of sea level rise from a sea level budget approach, Geophysical Research Letters, 44, 3744–3751, https://doi.org/10.1002/2017GL073308, 2017.

Dobslaw, H., Bergmann-Wolf, I., Dill, R., Poropat, L., Thomas, M., Dahle, C., Esselborn, S., König, R., and Flechtner, F.: A new high-resolution model of non-tidal atmosphere and ocean mass variability for de-aliasing of satellite gravity observations: AOD1B RL06, Geophysical Journal International, 211, 263–269, https://doi.org/10.1093/gji/ggx302, 2017.

Flechtner, F., Dobslaw, H., and Fagiolini, E.: GRACE AOD1B product description document for product release 05, 2014.

Frederikse, T., Riva, R., Kleinherenbrink, M., Wada, Y., van den Broeke, M., and Marzeion, B.: Closing the sea level budget on a regional scale: Trends and variability on the Northwestern European continental shelf, Geophysical Research Letters, 43, 10,864-10,872, https://doi.org/10.1002/2016GL070750, 2016.

Gregory, J. M., Griffies, S. M., Hughes, C. W., Lowe, J. A., Church, J. A., Fukimori, I., Gomez, N., Kopp, R. E., Landerer, F., Cozannet, G. L., Ponte, R. M., Stammer, D., Tamisiea, M. E., and van de Wal, R. S. W.: Concepts and Terminology for Sea Level: Mean, Variability and Change, Both Local and Global, Surv Geophys, 40, 1251–1289, https://doi.org/10.1007/s10712-019-09525-z, 2019.

Hamlington, B. D., Gardner, A. S., Ivins, E., Lenaerts, J. T. M., Reager, J. T., Trossman, D. S., Zaron, E. D., Adhikari, S., Arendt, A., Aschwanden, A., Beckley, B. D., Bekaert, D. P. S., Blewitt, G., Caron, L., Chambers, D. P., Chandanpurkar, H. A., Christianson, K., Csatho, B., Cullather, R. I., DeConto, R. M., Fasullo, J. T., Frederikse, T., Freymueller, J. T., Gilford, D. M., Girotto, M., Hammond, W. C., Hock, R., Holschuh, N., Kopp, R. E., Landerer, F., Larour, E., Menemenlis, D., Merrifield, M., Mitrovica, J. X., Nerem, R. S., Nias, I. J., Nieves, V.,

726 Nowicki, S., Pangaluru, K., Piecuch, C. G., Ray, R. D., Rounce, D. R., Schlegel, N.-J.,
727 Seroussi, H., Shirzaei, M., Sweet, W. V., Velicogna, I., Vinogradova, N., Wahl, T., Wiese, D.
728 N., and Willis, M. J.: Understanding of Contemporary Regional Sea-Level Change and the
729 Implications for the Future, Reviews of Geophysics, 58, e2019RG000672,
730 https://doi.org/10.1029/2019RG000672, 2020.
731 Horwath, M., Gutknecht, B. D., Cazenave, A., Palanisamy, H. K., Marti, F., Marzeion, B.,
732 Paul, F., Le Bris, R., Hogg, A. E., Otosaka, I., Shepherd, A., Döll, P., Cáceres, D., Müller
733 Schmied, H., Johannessen, J. A., Nilsen, J. E. Ø., Raj, R. P., Forsberg, R., Sandberg Sørensen,
734 L., Barletta, V. R., Simonsen, S. B., Knudsen, P., Andersen, O. B., Ranndal, H., Rose, S. K.,
735 Merchant, C. J., Macintosh, C. R., von Schuckmann, K., Novotny, K., Groh, A., Restano, M.,
736 and Benveniste, J.: Global sea-level budget and ocean-mass budget, with a focus on advanced
737 data products and uncertainty characterisation, Earth System Science Data, 14, 411–447,
738 https://doi.org/10.5194/essd-14-411-2022, 2022.
739 Liu, C., Liang, X., Chambers, D., and Ponte, R.: Global Patterns of Spatial and Temporal
740 Variability in Salinity from Multiple Gridded Argo Products, Journal of Climate,
741 https://doi.org/10.1175/JCLI-D-20-0053.1, 2020.
742 Llovel, W. and Hochet, A.: Salinity Contribution to Regional Sea Level Trends in the Tropical
743 Southwestern Pacific Ocean Over 2014–2023, Geophysical Research Letters, 52,
744 e2025GL116115, https://doi.org/10.1029/2025GL116115, 2025.
745 Llovel, W., Balem, K., Tajouri, S., and Hochet, A.: Cause of Substantial Global Mean Sea
746 Level Rise Over 2014–2016, Geophysical Research Letters, 50, e2023GL104709,
747 https://doi.org/10.1029/2023GL104709, 2023.
748 McDougall, T. J., Barker, P. M., Marine, CSIRO., and Research, A.: Getting started with
749 TEOS-10 and the gibbs seawater (GSW) oceanographic toolbox, Trevor J. McDougall, 2011.

Mu, D., Church, J. A., King, M., Ludwigsen, C. B., and Xu, T.: Contrasting Discrepancy in the Sea Level Budget Between the North and South Atlantic Ocean Since 2016, Earth and Space Science, 11, e2023EA003133, https://doi.org/10.1029/2023EA003133, 2024.

Nerem, R. S., Beckley, B. D., Fasullo, J. T., Hamlington, B. D., Masters, D., and Mitchum, G. T.: Climate-change–driven accelerated sea-level rise detected in the altimeter era, Proceedings of the National Academy of Sciences, 115, 2022–2025, https://doi.org/10.1073/pnas.1717312115, 2018.

Pardaens, A. K., Gregory, J. M., and Lowe, J. A.: A model study of factors influencing projected changes in regional sea level over the twenty-first century, Clim Dyn, 36, 2015–2033, https://doi.org/10.1007/s00382-009-0738-x, 2011.

Peltier, W. R., Argus, D. F., and Drummond, R.: Comment on "An Assessment of the ICE-6G_C (VM5a) Glacial Isostatic Adjustment Model" by Purcell et al.: The ICE-6G_C (VM5a) GIA model, J. Geophys. Res. Solid Earth, 123, 2019–2028, https://doi.org/10.1002/2016JB013844, 2018.

Ponte, R. M., Sun, Q., Liu, C., and Liang, X.: How Salty Is the Global Ocean: Weighing It All or Tasting It a Sip at a Time?, Geophysical Research Letters, 48, e2021GL092935, https://doi.org/10.1029/2021GL092935, 2021.

Roemmich, D. and Gilson, J.: The 2004–2008 mean and annual cycle of temperature, salinity, and steric height in the global ocean from the Argo Program, Progress in Oceanography, 82, 81–100, https://doi.org/10.1016/j.pocean.2009.03.004, 2009.

Royston, S., Dutt Vishwakarma, B., Westaway, R., Rougier, J., Sha, Z., and Bamber, J.: Can We Resolve the Basin-Scale Sea Level Trend Budget From GRACE Ocean Mass?, Journal of Geophysical Research: Oceans, 125, e2019JC015535, https://doi.org/10.1029/2019JC015535, 2020.

774 Storto, A. and Yang, C.: Acceleration of the ocean warming from 1961 to 2022 unveiled by
775 large-ensemble reanalyses, Nat Commun, 15, 545, https://doi.org/10.1038/s41467-024-44749-
776 7, 2024.
777 Sun, Y., Riva, R., and Ditmar, P.: Optimizing estimates of annual variations and trends in
778 geocenter motion and J_2 from a combination of GRACE data and geophysical models, J.
779 Geophys. Res. Solid Earth, 121, 8352–8370, https://doi.org/10.1002/2016JB013073, 2016.
780 Tapley, B., Watkins, M., Flechtner, F., Reigber, C., Bettadpur, S., Rodell, M., Sasgen, I.,
781 Famiglietti, J., Landerer, F., Chambers, D., Reager, J., Gardner, A., Save, H., Ivins, E.,
782 Swenson, S., Boening, C., Dahle, C., Wiese, D., Dobslaw, H., and Velicogna, I.: Contributions
783 of GRACE to understanding climate change, Nature Climate Change, 5,
784 https://doi.org/10.1038/s41558-019-0456-2, 2019.
785 Thierry, V., Claustre, H., Pasqueron De Fommervault, O., Zilberman, N., Johnson, K. S., King,
786 B. A., Wijffels, S. E., Bhaskar, U. T. V. S., Balmaseda, M. A., Belbeoch, M., Bollard, M.,
787 Boutin, J., Boyd, P., Cancouët, R., Chai, F., Ciavatta, S., Crane, R., Cravatte, S., Dall'Olmo,
788 G., Desbruyères, D., Durack, P. J., Fassbender, A. J., Fennel, K., Fujii, Y., Gasparin, F.,
789 González-Santana, A., Gourcuff, C., Gray, A., Hewitt, H. T., Jayne, S. R., Johnson, G. C.,
790 Kolodziejczyk, N., Le Boyer, A., Le Traon, P.-Y., Llovel, W., Lozier, M. S., Lyman, J. M.,
791 McDonagh, E. L., Martin, A. P., Meyssignac, B., Mogensen, K. S., Morris, T., Oke, P. R.,
792 Smith, W. O., Owens, B., Poffa, N., Post, J., Roemmich, D., Rykaczewski, R. R.,
793 Sathyendranath, S., Scanderbeg, M., Scheurle, C., Schofield, O., Von Schuckmann, K.,
794 Scourse, J., Sprintall, J., Suga, T., Tonani, M., Van Wijk, E., Xing, X., and Zuo, H.: Advancing
795 ocean monitoring and knowledge for societal benefit: the urgency to expand Argo to OneArgo
796 by 2030, Front. Mar. Sci., 12, 1593904, https://doi.org/10.3389/fmars.2025.1593904, 2025.
797 Wang, C., Dong, S., and Munoz, E.: Seawater density variations in the North Atlantic and the
798 Atlantic meridional overturning circulation, Clim Dyn, 34, 953–968,
799 https://doi.org/10.1007/s00382-009-0560-5, 2010.

WCRP: Global sea-level budget 1993–present, Earth System Science Data, 10, 1551–1590, https://doi.org/10.5194/essd-10-1551-2018, 2018.

Wong, A. P. S., Gilson, J., and Cabanes, C.: Argo salinity: bias and uncertainty evaluation, Earth System Science Data, 15, 383–393, https://doi.org/10.5194/essd-15-383-2023, 2023.

Wunsch, C., Ponte, R. M., and Heimbach, P.: Decadal Trends in Sea Level Patterns: 1993–2004, Journal of Climate, 20, 5889–5911, https://doi.org/10.1175/2007JCLI1840.1, 2007.

Zuo, H., Balmaseda, M. A., Tietsche, S., Mogensen, K., and Mayer, M.: The ECMWF operational ensemble reanalysis–analysis system for ocean and sea ice: a description of the system and assessment, Ocean Science, 15, 779–808, https://doi.org/10.5194/os-15-779-2019, 2019.